

Electronic Supplementary Information (ESI)

Thiophene-embedded Conjugated Microporous Polymers for Photocatalysis

Wan-Kai An,^{*a} Shi-Jia Zheng,^a Ya-Nan Du,^a San-Yuan Ding,^{*b} Zhi-Jun Li,^c Song Jiang,^a Yuchen Qin,^a Xiaobiao Liu,^a Pi-Feng Wei,^d Zhan-Qi Cao,^a Meirong Song,^a and Zhenliang Pan^{*a}

^aCollege of Science, Henan Agricultural University, Zhengzhou, Henan 450002, China. E-mail: anwk@henau.edu.cn, panzhenliang@sina.com.

^bState Key Laboratory of Applied Organic Chemistry, College of Chemistry and Chemical Engineering, Lanzhou University, Lanzhou, Gansu 730000, China. E-mail: dingsy@lzu.edu.cn

^cCollege of Chemistry and Chemical Engineering, Longdong University, Qingyang, Gansu 745000, China.

^dSchool of Chemistry & Chemical Engineering, Linyi University, Linyi, Shandong 276000, China.

List of Contents

1. Summary of Schemes and Figures	2
2. General Information	3
3. Synthetic Procedures	5
4. S_{BET} of TP-CMPs Prepared in Selected Conditions	7
5. Characterization of BTP-CMP and TBTP-CMP	7
6. Photocatalytic units in TP-CMPs	12
7. Typical Procedure for Photocatalytic Synthesis of 2-substituted Benzimidazoles	12
8. Scale-up Experiment for the Synthesis of 3a	14
9. Recyclability Tests of BTP-CMP	15
10. Study for the Reaction Mechanism	17
11. References	19
12. Liquid NMR Spectra of Some Compounds	20

1. Summary of Schemes and Figures

Scheme S1	Synthesis of TTDB and TBTP-2Br	S5
Scheme S2	Synthesis of TP-CMPs	S6
Table S1.	Condition optimization for BET surface areas of BTP-CMP	S7
Figure S1	FT-IR spectra of BTP-2Br and BTP-CMP	S7
Figure S2	FT-IR spectra of TBTP-2Br and TBTP-CMP.	S8
Figure S3	Optimized structures of the repeat units in TP-CMPs	S8
Figure S4	TGA curves of TP-CMPs	S9
Figure S5	Powder X-ray diffraction of TP-CMPs	S9
Figure S6	SEM images of TP-CMPs	S10
Figure S7	TEM images of TP-CMPs	S10
Figure S8	EDS analysis of TP-CMPs	S11
Figure S9	Cyclic voltammetry curves of TP-CMPs	S11
Figure S10	Proposed photocatalytic units within TP-based networks.	S12
Figure S11	Scale-up experiment of 3a with BTP-CMP as photocatalyst.	S14
Figure S12	Evaluation for the recyclability of BTP-CMP.	S15
Figure S13	N ₂ adsorption-desorption isotherms of fresh and recycled BTP-CMP	S15
Figure S14	FT-IR spectra of fresh and recycled BTP-CMP	S16
Figure S15	Liquid NMR spectra at different time intervals for the reaction system	S17
Figure S16	Cyclic voltammetry curves of imine I .	S18

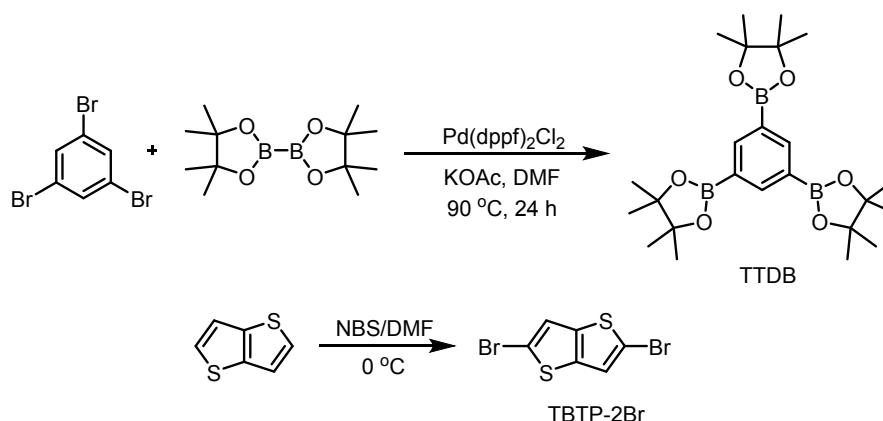
2. General Information

(1) Materials. 1,3,5-tris(4,4,5,5-tetramethyl-1,3,2-dioxaborolan-2-yl)benzene (TTDB)^[1], 2,5-dibromothiopheno[3,2-b]thiophene (TBTP-2Br)^[2] and were prepared according to the literature procedures. Other reagents can be purchased from commercial suppliers (Energy Chemical Reagent Co. Ltd and Adamas Reagent Co. Ltd) used without further purification, unless otherwise noted. N,N-dimethylformamide (DMF), N-methyl-pyrrolidone (NMP), N, N-dimethylacetamide (DMAc) were first dried by CaH₂ and further distilled before use. All Pd-mediated coupling reactions were carried out under Ar by using Schlenk line techniques. The deionized water was used during the synthesis of porous materials.

(2) Methods. Flash column chromatography was carried out with silica gel (200-300 mesh). Liquid NMR spectra (¹H and ¹³C) were recorded on a Bruker Avance III 400 MHz NMR spectrometer (CDCl₃ or d₆-DMSO as solvent). The chemical shifts δ and coupling constants J are given in ppm and Hz, respectively. Solid-state NMR experiments were performed on a Bruker WB Avance II 400 MHz NMR spectrometer (4-mm double-resonance probe). The parameters were set as following: contact time was 3 ms (ramp 100), recycle delay was 2 s and the spinning rate was 10,000 \pm 1 Hz. FT-IR spectra were obtained with a Nicolet IS 20 instrument. Powder X-ray diffraction (PXRD) data were collected with a PANalytical X'Pert Pro diffractometer operated at 40 kV and 40 mA with Cu K α radiation at a scan rate of 15 $^\circ$ /min. Nitrogen adsorption and desorption isotherms were measured at 77 K using a Micromeritics ASAP 2020M system. The samples were outgassed at 120 $^\circ$ C for 8 h before analysis. Surface areas were calculated based on the adsorption data via the Brunauer-Emmett-Teller (BET) and Langmuir methods, respectively. The pore-size-distribution (PSD) curves were obtained from the adsorption branches using non-local density functional theory (NLDFT) method. The pore volume was calculated from the amount of N₂ gas adsorbed at p/p₀ = 0.99 based on the t-plot analysis. Thermogravimetric analysis (TGA) measurements were used to study the thermal stability of the porous organic polymers. The tests were carried out on a SDT Q600 (V20.9 Build 20) instrument from 35 to 1000 $^\circ$ C under a N₂ atmosphere with a heating rate of 10 $^\circ$ C/min. Elemental analysis was performed on a Vario EL cube instrument. Scanning electron microscope (SEM) tests were applied to analysis the surface morphologies and microstructures of the obtained materials with Zeiss GeminiSEM 500 at a voltage of 15 kV. The samples used for SEM analysis were dispersed in ethanol, and then dipped and dried on a silicon wafer. To detect the

elemental compositions within the porous networks, part regions in SEM analytical samples were selected to collect the Energy-dispersive X-ray spectroscopic (EDS) data at a voltage of 15 kV. High resolution transmission electron microscopy (HR-TEM) images were acquired by a Tecnai G2 F30 transmission electron microscope (FEI, USA) operating at an acceleration voltage of 300 kV. The porous materials dispersed in ethanol were dipped and dried on copper meshes before TEM analysis. The palladium contents of the polymeric samples were determined by inductively coupled plasma (ICP) analysis with a TJA IRIS Advantage ER/S instrument. UV-Vis diffuse reflectance analysis (for solid samples) was recorded on a JASCO model V-670 spectrometer equipped with integration sphere model IJN-727. The bandgaps were estimated from the UV-Vis diffuse reflectance spectra through Kubelka-Munk function. Cyclic voltammetry (CV) experiments were conducted on CHI660C Electrochemical Workstation potentiostat (Shanghai Chen Hua Electrochemical Instrument) by using a three-electrode (a glassy-carbon working electrode, a saturated calomel reference electrode and a platinum wire counter electrode) electrochemical cell. First, the working electrode was polished with 0.05 μm $\text{Al}_2\text{O}_3\text{-H}_2\text{O}$ slurry on a felt surface before washing with ultrapure water. After dispersing the fine solid powder (5.0 mg) into ethanol (0.5 mL) and ultrasound for 1h, the electrode could be obtained through drop-casting the slurry onto the working electrode, and then dried under air. In addition, 5 % Nafion will be used if necessary. All the CV measurements were performed at a scan rate of 100 mV/s in degassed acetonitrile solution that contain Bu_4NPF_6 (0.1 M).

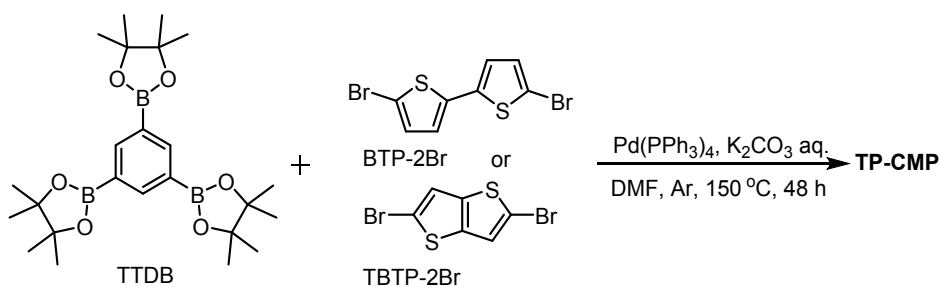
3. Synthetic Procedures



Scheme S1. Synthesis of TTDB and TBTP-2Br.

Synthesis of TTDB.^[1] 1,3,5-tribromobenzene (1.5 g, 4.76 mmol), bis(pinacolato)diboron (3.81 g, 14.30 mmol), potassium acetate (2.80 g, 28.5 mmol) and Pd(dppf)Cl₂ (131 mg, 0.18 mmol) were added into an oven-dried 50 mL two-neck flask. The system was degassed and back-filled with nitrogen for three times, and then anhydrous DMF (15 mL) was added under nitrogen atmosphere. The reaction was stirred at 90 °C for 24 h. The mixture was poured into deionized water (200 mL) after the reaction system was cooled down to room temperature. The obtained brownish black solid was collected by filtration and washed with plenty of water. After drying under vacuum at 60 °C for 5 h, the crude product was purified through recrystallization with methanol and give white solid product TTDB (1.3 g, 62% yield). ¹H NMR (400 MHz, CDCl₃): δ ppm 8.36 (s, 3H), 1.33 (s, 36H); ¹³C NMR (100 MHz, CDCl₃): δ (ppm) 144.1, 83.7, 24.9.

Synthesis of monomer TBTP-2Br.^[2] N-Bromosuccinimide (3.58 g, 20 mmol) was added slowly into a stirred solution of thieno[3,2-b] thiophene (1.40 g, 10 mmol) in N,N-dimethylformamide (DMF, 20 mL) under 0 °C. The system was stirred for 3 h at room temperature and then water was added to quench the reaction. The mixture was extracted with diethyl ether, and the collected organic phase was dried over anhydrous Na₂SO₄. After removing the excess solvent under reduced pressure, the crude product was purified by flash silica gel column chromatography using petroleum ether as the eluent to give product TBTP-2Br as white solid (2.4 g, 80% yield). ¹H NMR (400 MHz, CDCl₃): δ ppm 7.17 (s, 2H); ¹³C NMR (100 MHz, CDCl₃): δ (ppm) 138.3, 121.8, 113.6.



Scheme S2. Synthesis of TP-CMPs.

Synthesis of BTP-CMP and TBTP-CMP. BTP-CMP and TBTP-CMP were prepared via Suzuki-Miyaura coupling reaction. A two-necked flask was charged with TTDB (182.4 mg, 0.4 mmol), dibromo-substituted thiophene derivatives BTP-2Br (194.4 mg, 0.6 mmol) or TBTP-2Br (178.8 mg, 0.6 mmol), Pd(PPh₃)₄ (18.4 mg, 0.016 mmol). And then DMF (16 mL) and 2 M K₂CO₃ aqueous solution (3.2 mL) were added into the flask. The reaction mixture was stirred and bubbled by Ar ball for 30 minutes at room temperature. Then, the system was stirred under 150 °C and Ar atmosphere for 48 h. After cooling to ambient temperature, the precipitate was filtrated and washed in turn with deionized water, DMF, EtOH, dichloromethane and acetone. The resulting solid was further purified by the Soxhlet extraction for 24 h with THF and acetone as solvent, respectively. After drying in vacuum for 12 h at 80 °C, the conjugated microporous polymers were obtained as deep-yellow powder. **BTP-CMP**: 122 mg, 95% yield. Anal. Calcd for (C₃₆H₁₈S₆)_n (%): C, 67.29; H, 2.80; S, 29.91 ; Found C, 66.02; H, 2.27; S, 28.84. **TBTP-CMP**: 115 mg, 93% yield. Anal. Calcd for (C₃₀H₁₂S₆)_n (%): C, 63.83; H, 2.13; S, 34.04; Found C, 62.71; H, 2.02; S, 32.71. As identified by ICP analysis, the residual Pd contents within polymeric networks was 0.686% and 0.629% for BTP-CMP and TBTP-CMP, respectively.

4. S_{BET} of TP-CMPs Prepared in Selected Conditions

Table S1. Summary of S_{BET} for TP-CMPs prepared in different conditions.

TP-CMPs	Solvent	T (°C)	yield (%)	S_{BET} ($\text{m}^2 \text{g}^{-1}$)
BTP-CMP	DMF	150	95	242
	THF	80	98	36
	1,4-Dioxane	120	86	45
	NMP	150	92	50
	DMAc	150	94	32
	Toluene	100	52	19
	DMF	130	96	176
TBTP-CMP	DMF	150	93	571
	DMAc	150	95	222

General conditions: TTDB (0.4 mmol), BTP-2Br or TBTP-2Br (0.6 mmol), $\text{Pd}(\text{PPh}_3)_4$ (0.016 mmol), solvent (16 mL), 2 M K_2CO_3 aqueous solution (3.2 mL), Ar, 48 h. S_{BET} : BET surface area.

5. Characterization of BTP-CMP and TBTP-CMP

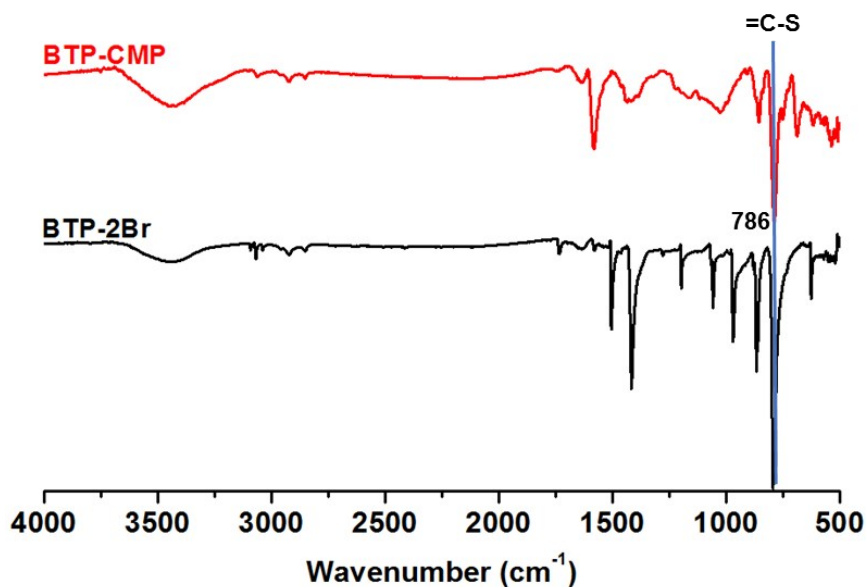


Figure S1. FT-IR spectra of BTP-2Br and BTP-CMP.

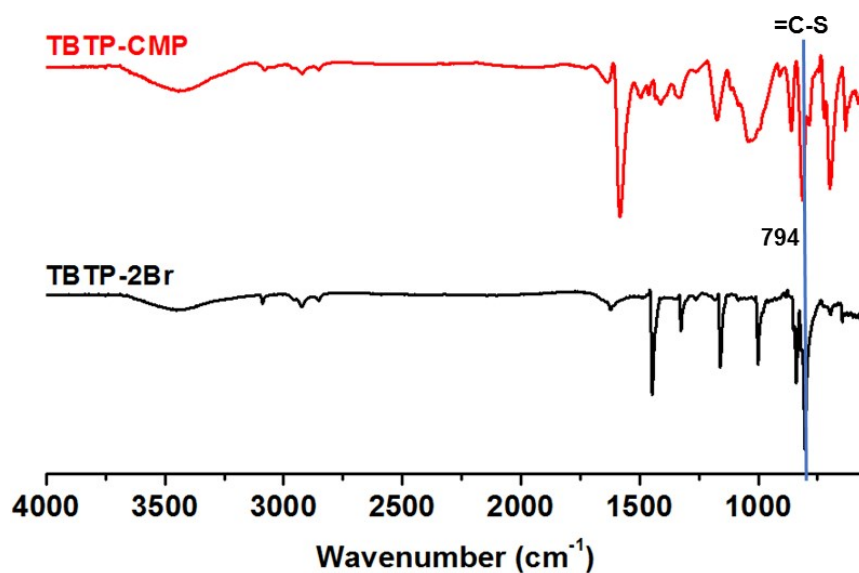


Figure S2. FT-IR spectra of TBTP-2Br and TBTP-CMP.

The FT-IR spectra (Figure S1 and S2) of TP-CMP showed peaks at about 790 cm^{-1} , which demonstrated the presence of =C-S bonds that come from thiophene units. The signal imply that 2,2'-bithiophene and thieno[3,2-b]thiophene was incorporated into the networks of BTP-CMP and TBTP-CMP, respectively.

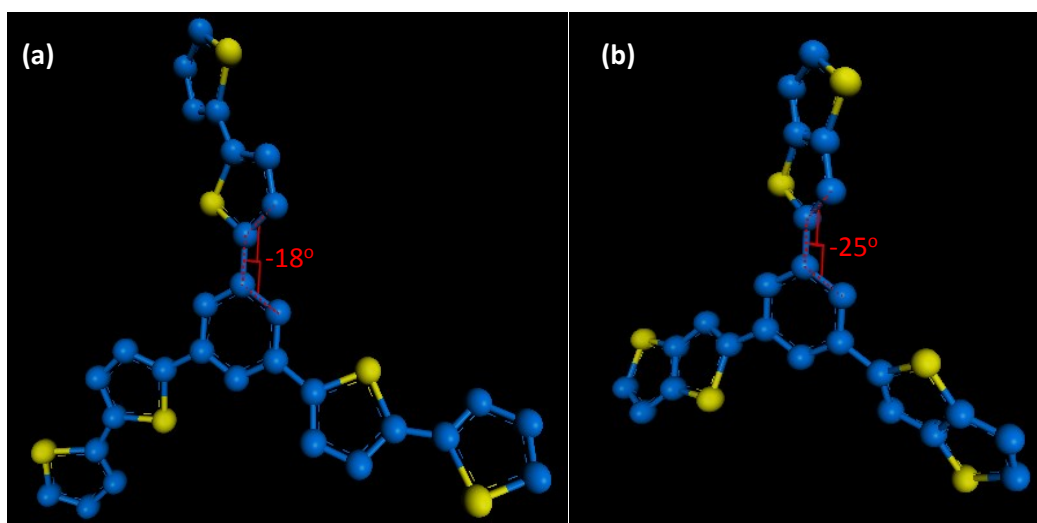


Figure S3. Optimized structures (DFT method) of repeat units for BTP-CMP (a) and TBTP-CMP (b).

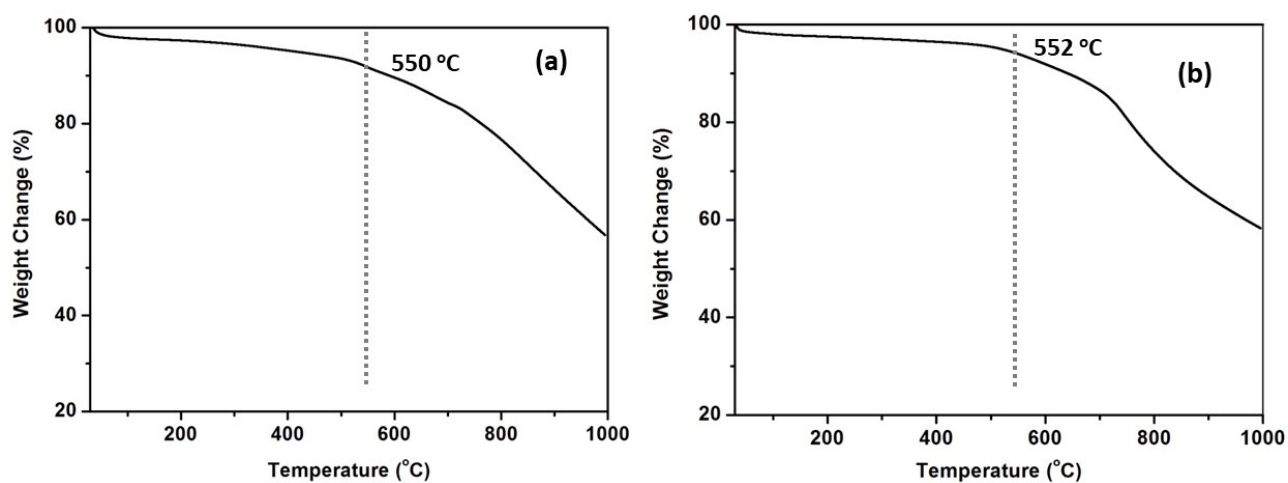


Figure S4. TGA curves of BTP-CMP and TBTP-CMP. As shown in Figure S4, the two porous networks were enough stable up to about 550 °C and with leftover weight of 57% under N₂ atmosphere.

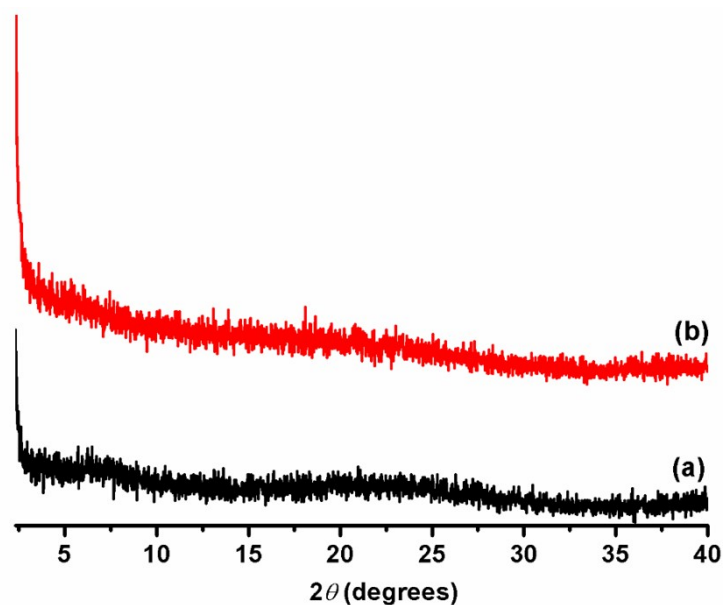


Figure S5. Powder X-ray diffraction of BTP-CMP (a) and TBTP-CMP (b). These results proved that both BTP-CMP and TBTP-CMP were amorphous materials.

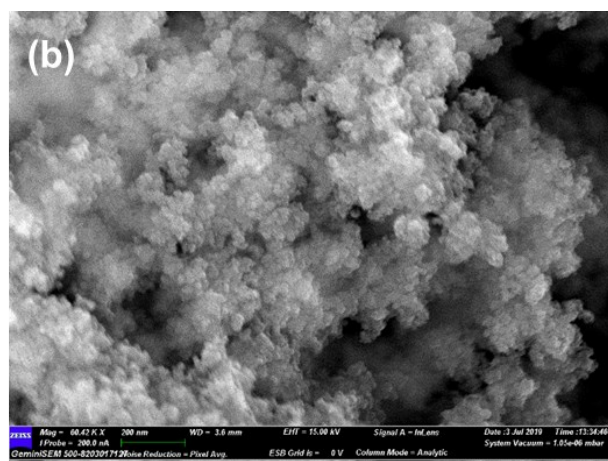
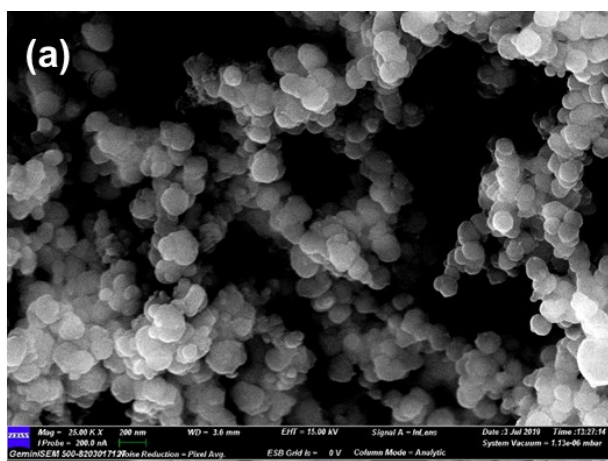


Figure S6. SEM images of BTP-CMP (a) and TBTP-CMP (b)

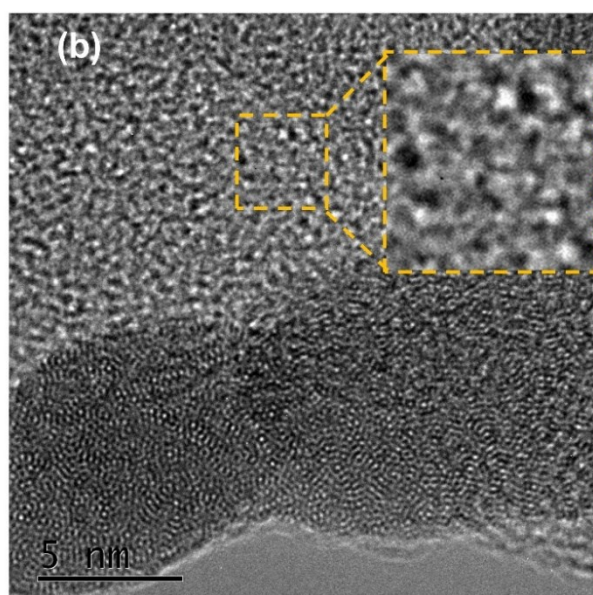
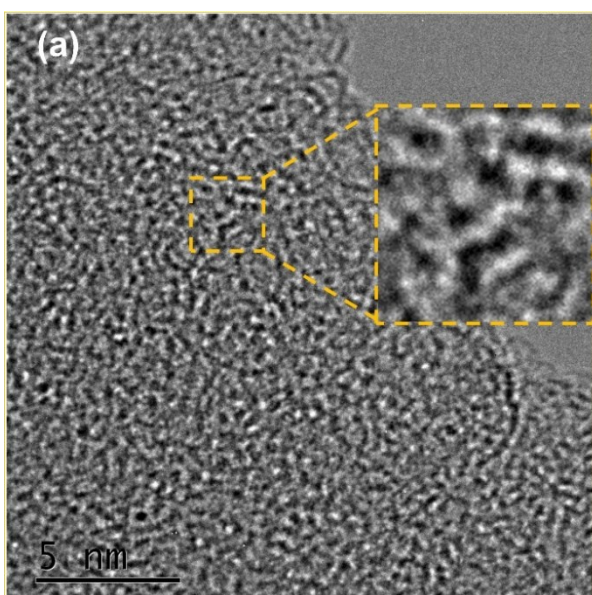


Figure S7. TEM images of BTP-CMP (a) and TBTP-CMP (b).

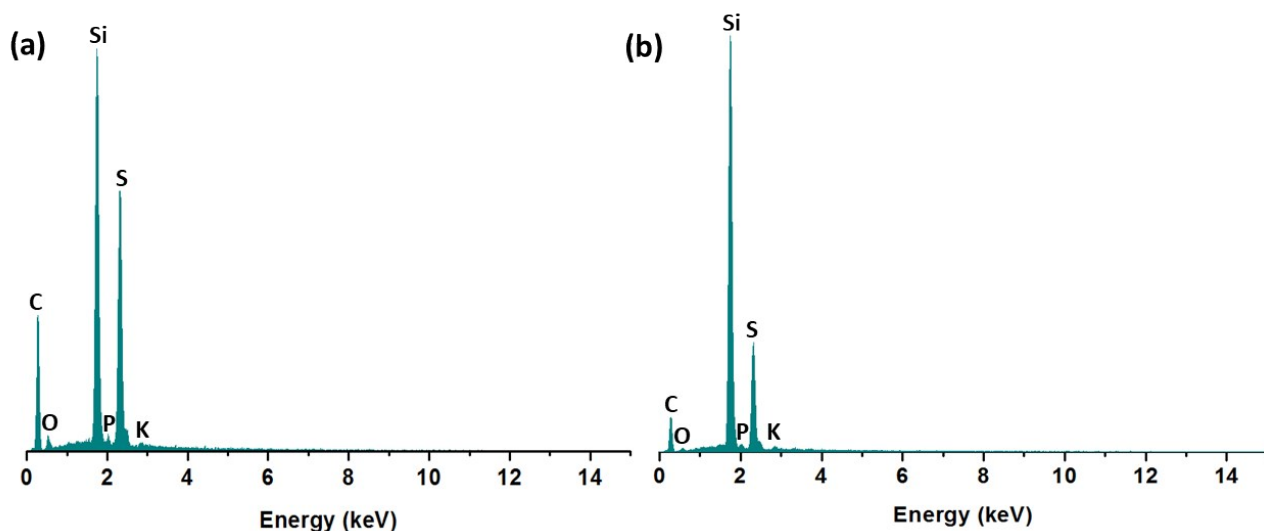


Figure S8. EDS analysis of BTP-CMP (a) and TBTP-CMP (b). The data was collected through SEM analysis in the selected area. C (70.5% for BTP-CMP, 65.4 % for TBTP-CMP) and S (23.7% for BTP-CMP, 29.5 % for TBTP-CMP) content were detected within the two polymeric porous frameworks. The O, K and P trace in BTP-CMP and TBTP-CMP can be attributed to the residual K_2CO_3 and decomposed $Pd(PPh_3)_4$. The silicon content herein came from silicon wafer used in SEM analysis.

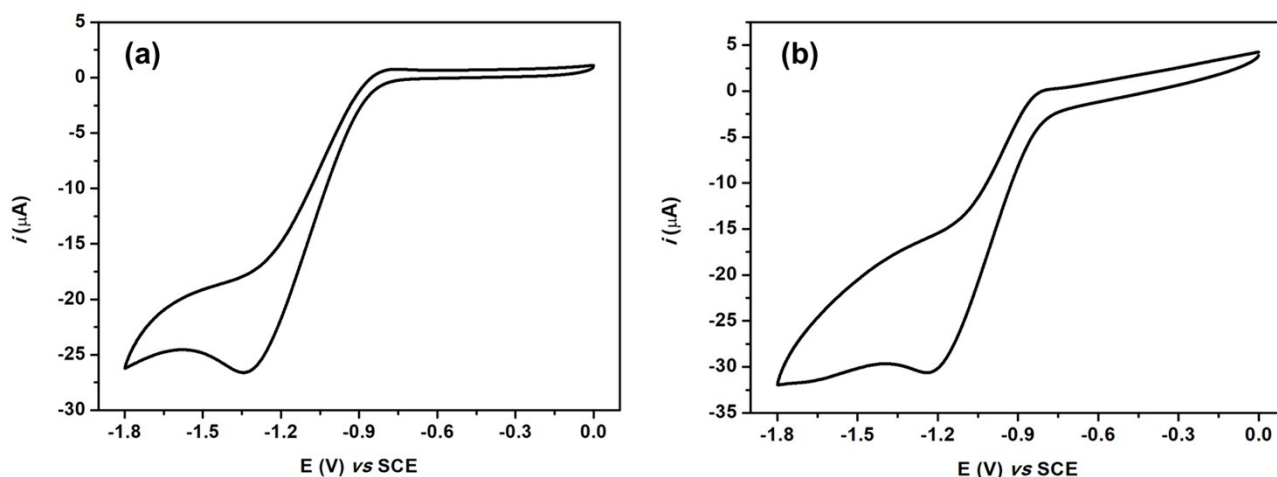


Figure S9. Cyclic voltammetry curves of BTP-CMP (a) and TBTP-CMP (b). The experiments were conducted in anhydrous acetonitrile solution of Bu_4NPF_6 (0.1 M) at a scan rate of 0.1 V/s. According to Figure S8, the conduction band positions (vs. SCE) for BTP-CMP and TBTP-CMP could be estimated as -0.92 V and -0.88 V, respectively.

6. Photocatalytic units in TP-CMPs

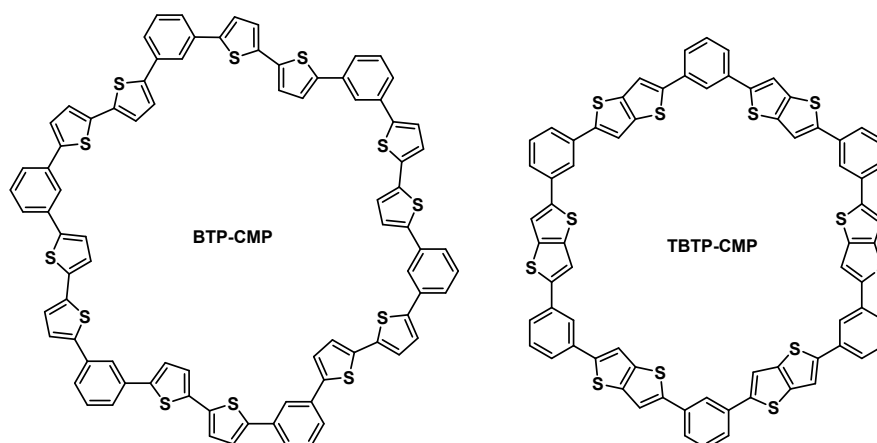
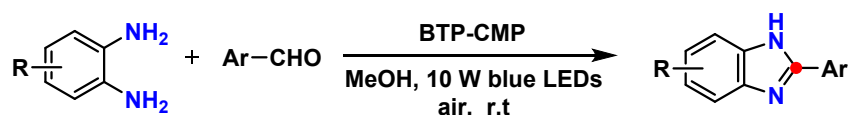
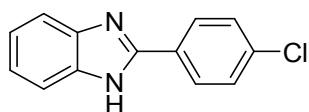


Figure S10. Proposed photocatalytic units within TP-based networks. In order to evaluate the catalyst loading, corresponding conjugate macrocycles were selected as the repeat catalytic units.^[3]

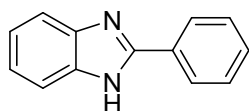
7. Typical Procedure for Photocatalytic Synthesis of 2-substituted Benzimidazoles



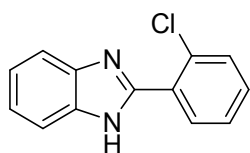
BTP-CMP (12 mg, 4.2 mol%), benzene-1,2-diamine or its derivatives (0.2 mmol), aromatic aldehyde (0.2 mmol) and MeOH (4.0 mL) were added into a reaction tube. The reaction mixture was opened to air and stirred at room temperature under 10 W blue LEDs (the distance between LEDs and reaction tube is about 10 cm). After the reaction was completed (monitored by TLC), the heterogeneous catalyst could be isolated through centrifugation and thoroughly washed by acetone (4 mL \times 3). After the organic solvent was removed at reduced pressure, the resulted crude product was further purified by flash column chromatography (with petroleum/acetone = 10/1~5/1 as eluent) to give 2-substituted benzimidazole.



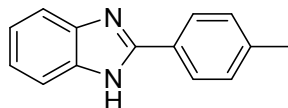
White solid, 98 % yield. ¹H NMR (400 MHz, *d*₆-DMSO): δ = 13.02 (br, 1H), 8.20 (d, *J* = 8.6 Hz, 2H), 7.63 (d, *J* = 8.6 Hz, 3H), 7.57-7.55 (m, 1H), 7.22-7.21 (m, 2H) ppm.



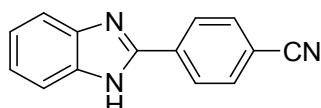
White solid, 93 % yield. ¹H NMR (400 MHz, *d*₆-DMSO): δ = 12.92 (br, 1H), 8.20-8.18 (m, 2 H), 7.67(d, *J* = 7.3 Hz, 1H), 7.58-7.54 (m, 3H), 7.51-7.47 (m, 1H), 7.24-7.17(m, 2H) ppm.



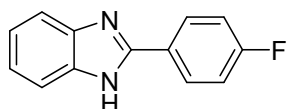
White solid, 91 % yield. $^1\text{H NMR}$ (400 MHz, CDCl_3): $\delta = 10.40$ (br, 1H), 8.42, 8.40 (dd, $J = 7.4$ Hz, 2.3 Hz, 1H), 7.86-7.84 (m, 1H), 7.53-7.48 (m, 2H), 7.44-7.36 (m, 2H), 7.33-7.29 (m, 2H) ppm.



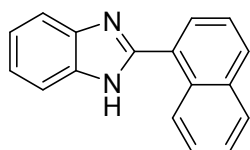
Light brown solid, 96 % yield. $^1\text{H NMR}$ (400 MHz, d_6 -DMSO): $\delta = 12.83$ (br, 1H), 8.08 (d, 8.1 Hz, 2H), 7.64 (s, 1H), 7.52 (s, 1H), 7.35 (d, $J = 8.0$ Hz, 2H), 7.19 (d, $J = 4.5$ Hz, 2H), 2.38 (s, 3H) ppm.



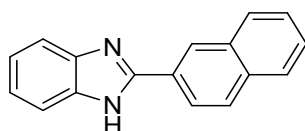
Orange-yellow solid, 92 % yield. $^1\text{H NMR}$ (400 MHz, CDCl_3): $\delta = 10.00$ (br, 1H), 8.17 (d, $J = 8.4$ Hz, 2H), 7.84-7.81 (m, 1H), 7.78 (d, $J = 8.4$ Hz, 2H), 7.52 (s, 1H), 7.35-7.31 (m, 2H).



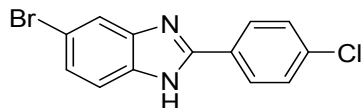
White solid, 94 % yield. $^1\text{H NMR}$ (400 MHz, d_6 -DMSO): $\delta = 12.94$ (br, 1H), 8.27-8.22 (m, 2H), 7.78 (d, $J = 7.4$ Hz, 1H), 7.55 (d, $J = 7.3$ Hz, 1H), 7.45-7.39 (m, 2H), 7.25-7.18 (m, 2H) ppm.



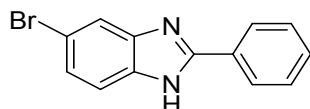
White solid, 94 % yield. $^1\text{H NMR}$ (400 MHz, d_6 -DMSO): $\delta = 12.96$ (br, 1H), 9.14 ($J = 8.3$ Hz, 1H), 8.10 (d, $J = 8.2$ Hz, 1H), 8.06-8.03 (m, 2H), 7.80 (d, $J = 7.5$ Hz, 1H), 7.71-7.59 (m, 4H), 7.31-7.24 (m, 2H).



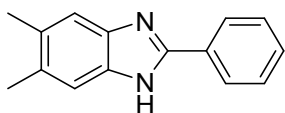
White solid, 92 % yield. $^1\text{H NMR}$ (400 MHz, d_6 -DMSO): $\delta = 13.09$ (br, 1H), 8.76 (s, 1H), 8.34, 8.32 (dd, $J = 8.6$ Hz, 1.7 Hz, 1H), 8.09-8.04 (m, 2H), 7.99-7.97 (m, 1H), 7.72 (d, $J = 7.5$ Hz, 1H), 7.63-7.57 (m, 3H), 7.27-7.20 (m, 2H) ppm.



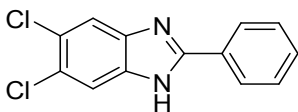
White solid, 97 % yield. $^1\text{H NMR}$ (400 MHz, CDCl_3): $\delta = 10.34$ (br, 1H), 7.20-7.14 (m, 4H), 7.74 (s, 1H), 7.45-7.42 (m, 2H), 7.39, 7.37 (d, $J = 1.76$ Hz, 1H) ppm.



Light brown solid, 98 % yield. $^1\text{H NMR}$ (400 MHz, d_6 -DMSO): $\delta = 13.13$ (br, 1H), 8.19-8.16 (m, 2H), 7.79 (s, 1H), 7.58-7.49 (m, 4H), 7.35, 7.33 (dd, $J = 8.5$ Hz, 1.9 Hz, 1H) ppm.



White solid, 96 % yield. $^1\text{H NMR}$ (400 MHz, CDCl_3): $\delta = 12.63$ (br, 1H), 8.14 (d, $J = 7.4$ Hz 2H), 7.54-7.51 (t, 2H), 7.47-7.44 (t, 1H), 7.36 (s, 2H), 2.32 (s, 6H) ppm.



White solid, 96 % yield. $^1\text{H NMR}$ (400 MHz, CDCl_3): $\delta = 13.25$ (br, 1H), 8.17 (d, $J = 5.8$ Hz 2H), 7.94 (s, 1H), 7.76 (s, 1H), 7.57-7.55 (m, 3H) ppm.

8. Scale-up Experiment for the Synthesis of **3a**

Benzene-1,2-diamine **1a** (540.7 mg, 5 mmol), 4-chlorobenzaldehyde **2a** (702.8 mg, 5 mmol), BTP-CMP (180 mg, 2.5 mol%) and MeOH (100 mL) were added into a reaction bottle. The reaction mixture was opened to air and stirred at room temperature under 10 W blue LEDs (the distance between LEDs and reaction center is about 10 cm). After the reaction was completed (ca. 5 hours, monitored by TLC), the heterogeneous catalyst could be isolated through filtration and thoroughly washed by acetone (10 mL \times 3). Collected the light brown mother liquid and removed the organic solvent under reduced pressure. The resulted crude product was further washed with a small amount of cold petroleum ether /EtOH (v/v, 10/1), and then dried under vacuum for 12 h at 80 $^\circ\text{C}$ to give pure **3a** as off-white solid (1.06 g, 93% yield).

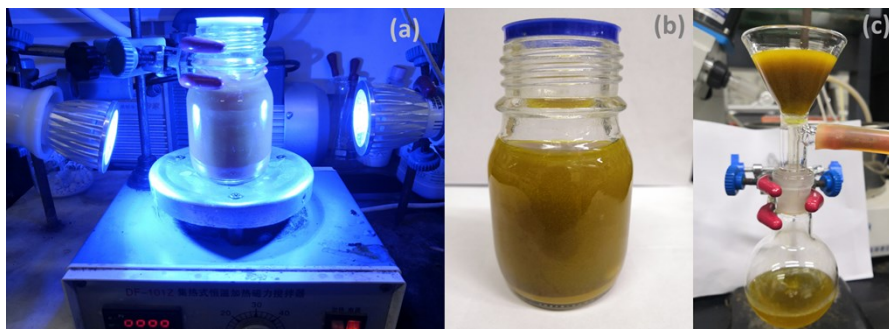


Figure S11. Scale-up experiment of **3a** with BTP-CMP as photocatalyst. (a) Photocatalytic reaction equipment (5 W \times 2 blue LEDs). (b) The completed reaction system that contain product **3a** and BTP-CMP catalyst; (c) Separation of **3a** and recovery of BTP-CMP through filtration.

9. Recyclability Tests of BTP-CMP

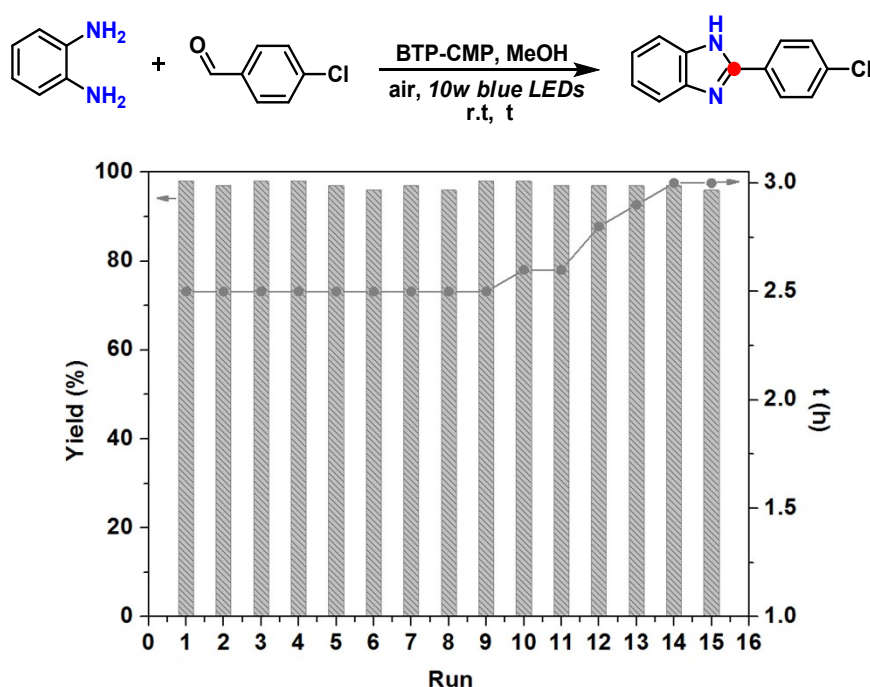


Figure S12. Evaluation for the recyclability of BTP-CMP. All the recycling experiments were performed under the identical conditions as described in Table 1, entry 12. Benzene-1,2-diamine (0.2 mmol), 4-chlorobenzaldehyde (0.2 mmol), MeOH (4.0 mL). The isolated yields were given for all runs.

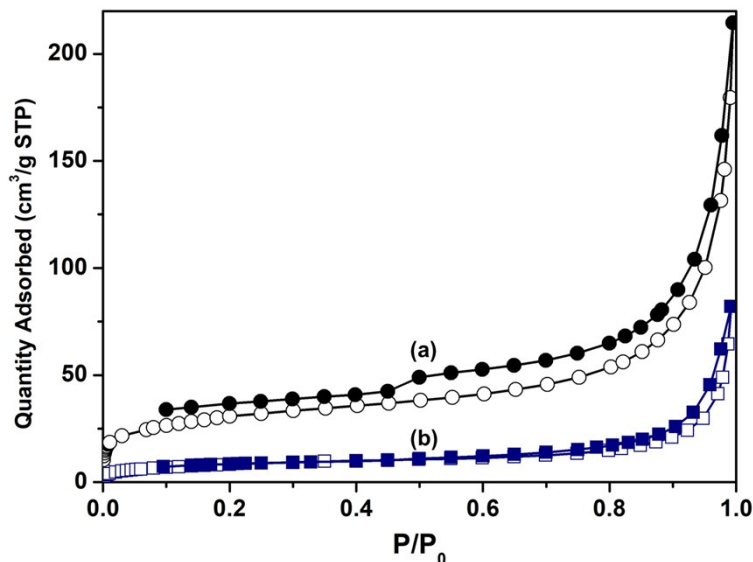


Figure S13. N₂ adsorption-desorption isotherms of fresh BTP-CMP (a, BET surface area of 242 m² g⁻¹) and the recycled BTP-CMP after the 15th run (b, BET surface area of 30 m² g⁻¹). STP = standard temperature and pressure.

As shown in Figure S12, the **BTP-CMP** could even remain a good catalytic activity after 15th run, though the reaction rate tended to be slow with the increase of recycling time. In combination with the nitrogen desorption tests (Figure S13) of the recycled catalyst, a clear finding here was that

the BET surface areas of porous organic polymers were crucial for excellent catalytic effects.

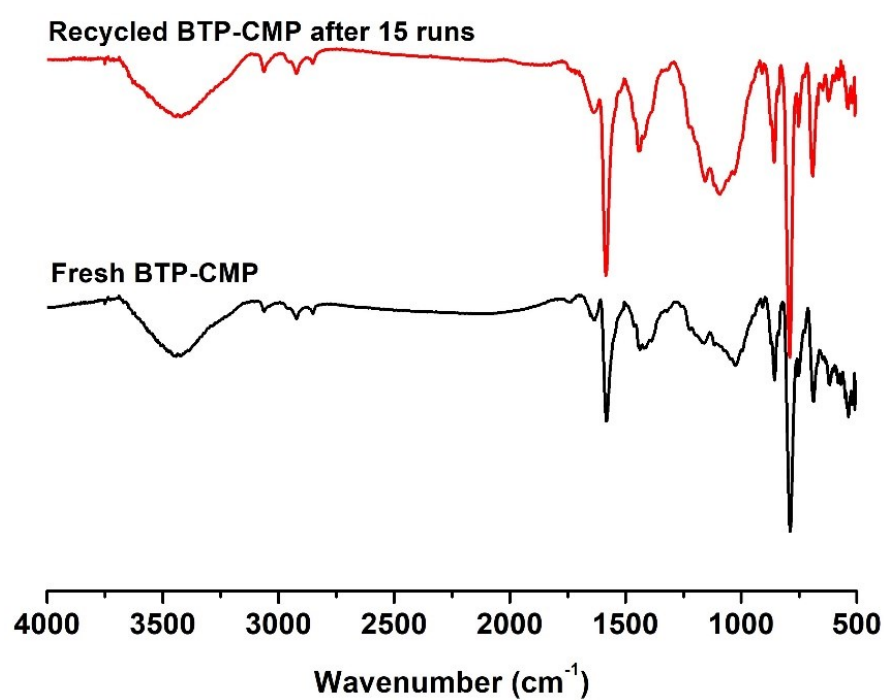


Figure S14. FT-IR spectra of fresh and recycled BTP-CMP.

10. Study for the Reaction Mechanism

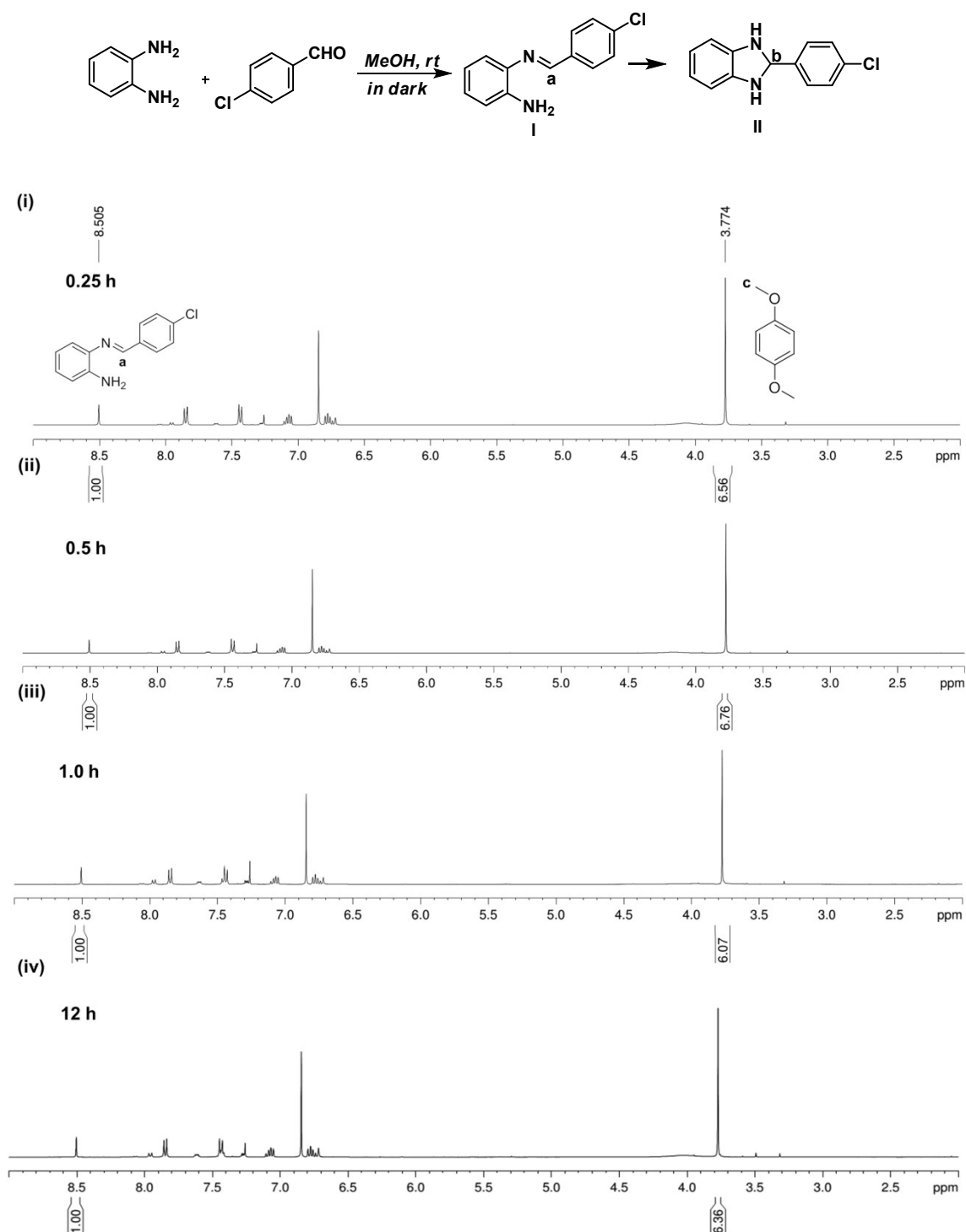


Figure S15. Liquid NMR spectra (CDCl_3 as NMR solvent, 1,4-dimethoxybenzene as internal standard compound) at different time intervals for the reaction system of benzene-1,2-diamine and 4-chlorobenzaldehyde.

Control reactions were carried out according to the following procedures: benzene-1,2-diamine (0.2 mmol) and 4-chlorobenzaldehyde (0.2 mmol) were first dissolved in MeOH (4.0 mL), and then closed the reaction tube. The mixtures were stirred for a period of appropriate time in the dark

before 1,4-dimethoxybenzene (m_0 mg) was added and then dissolved sufficiently. After that, the excess solvent was removed under vacuum at 25 °C to afford the yellow oil that contain internal standard reagent. The obtained mixtures were dissolved again in CDCl_3 and tested immediately via NMR. ^1H NMR (CDCl_3)^[4]: $\delta = 8.505$ ppm (s, H_a from imine **I**), 5.337 ppm (s, H_b from aminal **II**), 3.774 ppm (s, H_c from 1,4-dimethoxybenzene). The signal of H_a was very obvious, while H_b was so weak that aminal **II** almost could not be found. The yield of intermediates can be calculated as:

$$\text{yield (\%)} = \frac{6m_0S_x}{0.2 \cdot M_0S_0} \times 100$$

m_0 (mg): the mass of 1,4-dimethoxybenzene (27.8 mg);

M_0 (g/mol): molecular weight of 1,4-dimethoxybenzene (138.07 g/mol);

S_0 : the relative integration value for the peak area of the $-\text{OCH}_3$ in 1,4-dimethoxybenzene;

S_x : the relative integration value for the peak area of the imine groups (H_a) in **I**.

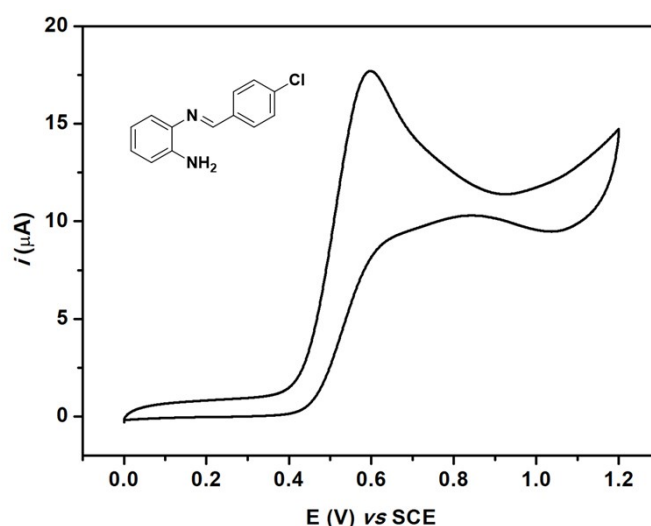


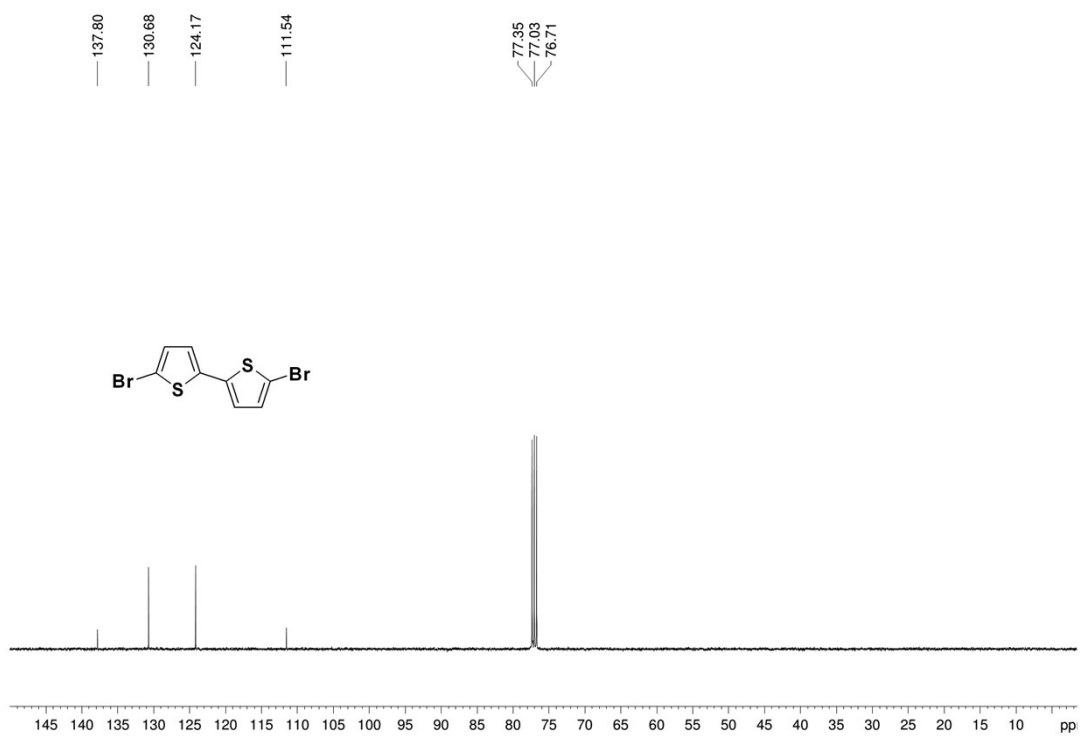
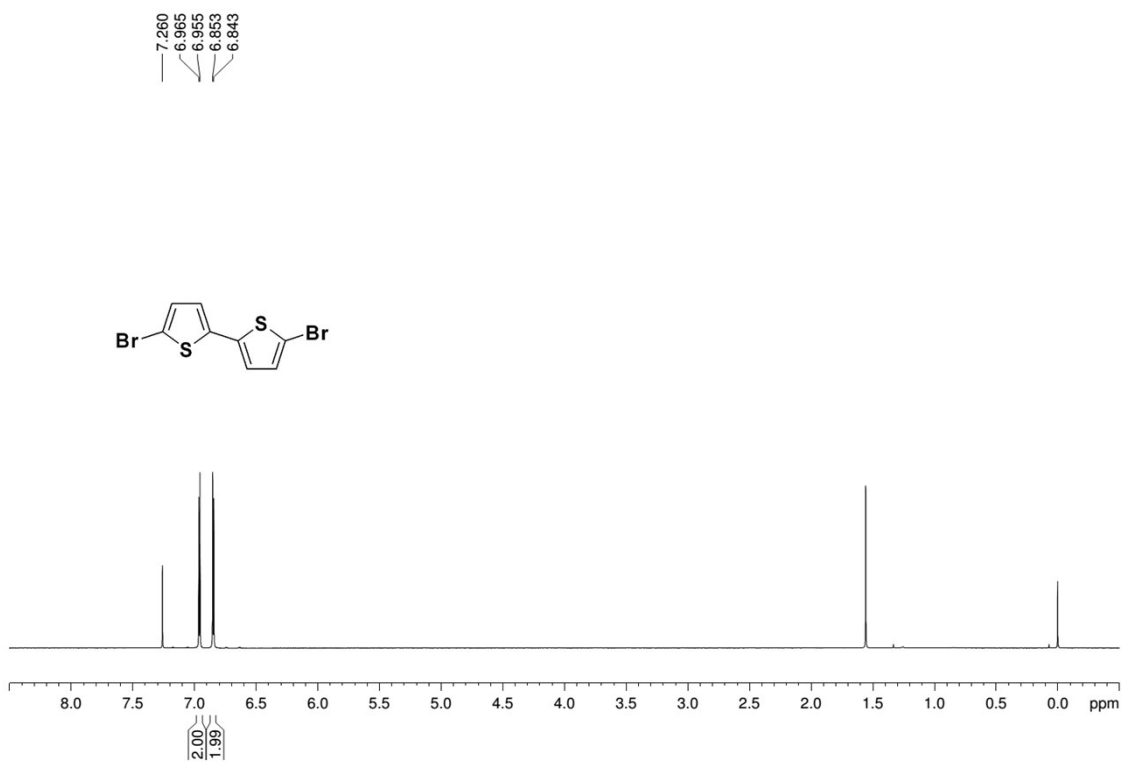
Figure S16. Cyclic voltammetry curves of imine **I**.

The experiment was conducted in anhydrous acetonitrile solution of Bu_4NPF_6 (0.1 M) at a scan rate of 0.1 V/s. Based on the figure above, the redox potential (vs. SCE) of **I** could be estimated as 0.45 V.

11. References

1. (a) Y.-B. Zhang, H. Furukawa, N. Ko, W. Nie, H. J. Park, S. Okajima, K. E. Cordova, H. Deng, J. Kim and O. M. Yaghi, *J. Am. Chem. Soc.*, **2015**, *137*, 2641-2650; (b) J. M. Tobin, J. Liu, H. Hayes, M. Demleitner, D. Ellis, V. Arrighi, Z. Xu and F. Vilela, *Polym. Chem.*, **2016**, *7*, 6662-6670.
2. M. Dogru, M. Handloser, F. Auras, T. Kunz, D. Medina, A. Hartschuh, P. Knochel and T. Bein, *Angew. Chem. Int. Edit.*, **2013**, *52*, 2920-2924.
3. P.-F. Wei, M.-Z. Qi, Z.-P. Wang, S.-Y. Ding, W. Yu, Q. Liu, L.-K. Wang, H.-Z. Wang, W.-K. An and W. Wang, *J. Am. Chem. Soc.*, **2018**, *140*, 4623-4631.
4. Z. Li, H. Song, R. Guo, M. Zuo, C. Hou, S. Sun, X. He, Z. Sun and W. Chu, *Green Chem.*, **2019**, *21*, 3602-3605.

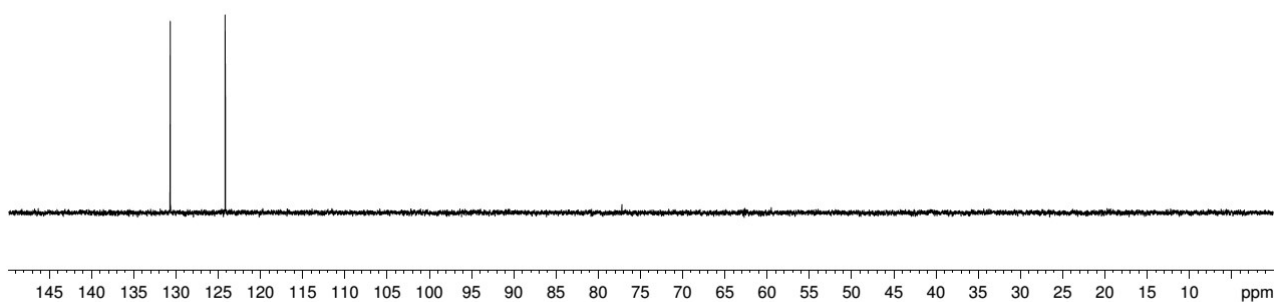
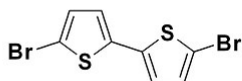
12. Liquid NMR Spectra of Some Compounds



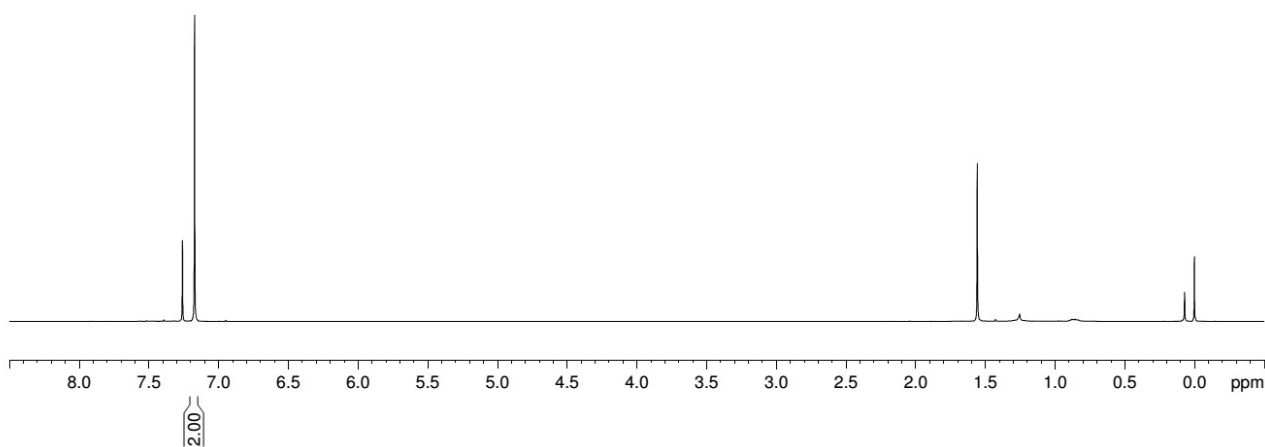
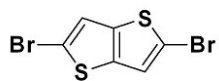
130.68
124.17

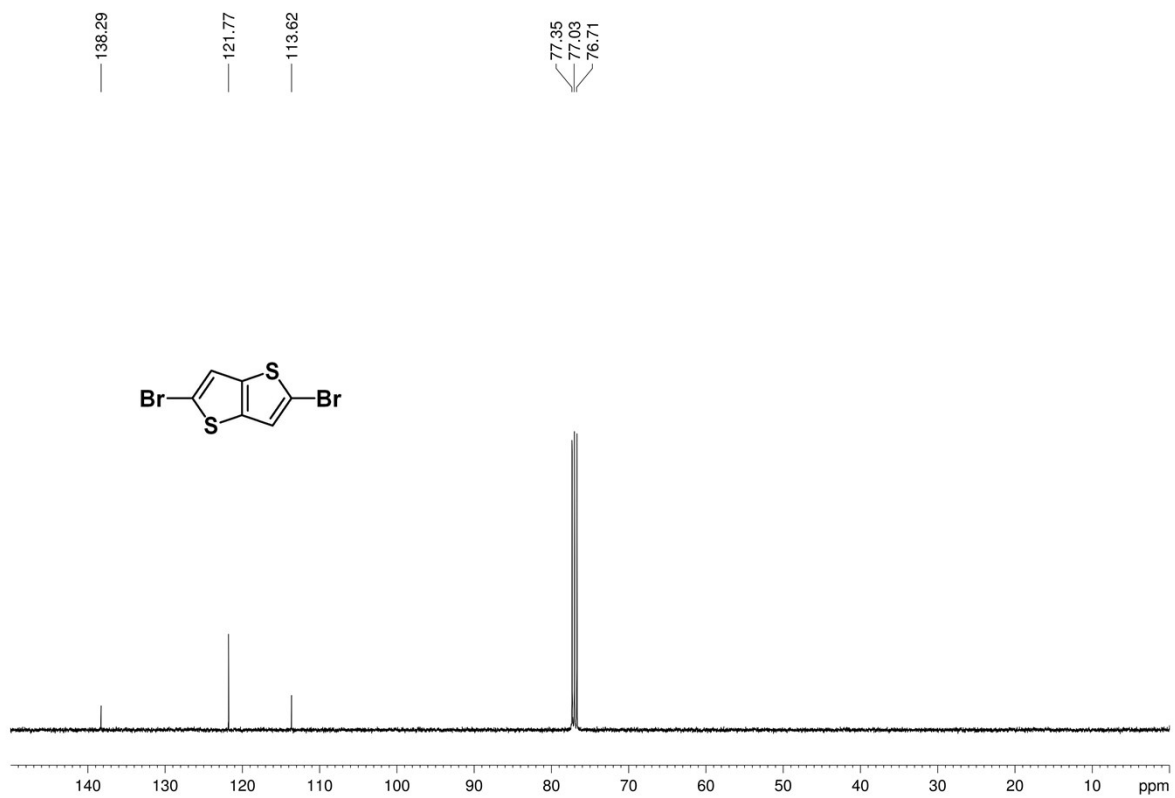
77.23

Depts 135



7.260
7.173





121.77

77.23

Deptsp135

